Structure of Glyoxal Dihydrazone and Synthesis, Characterization, and Iodine Doping of Unsubstituted Polyazine

Benjamin Chaloner-Gill,† Clair J. Cheer,† James E. Roberts,*,‡ and William B. Euler*,†

Department of Chemistry, University of Rhode Island, Kingston, Rhode Island 02881, and Department of Chemistry, Lehigh University, Seeley G. Mudd Building 6, Bethlehem, Pennsylvania 18015

Received April 12, 1990

ABSTRACT: The unsubstituted polyazine, $-[N{=}CH{-}CH{=}N]_x-$, has been synthesized from glyoxal dihydrazone and glyoxal. An X-ray crystal structure was done on the monomer glyoxal dihydrazone; it crystallized in space group $P2_1/a$ with cell constants $a = 7.744$ (4) Å, $b = 4.113$ (1) Å, $c = 8.063$ (4) Å, and $\beta = 115.66$ (3)° and $Z = 2$; intensity data were collected in the range $3.5 \leq 2\theta \leq 60°$. Refinement to convergence of the 683 independent reflections, $I > 3\sigma(I)$, resulted in final anisotropic $R = 0.056$ and $R_w = 0.059$. The monomer is planar with a carbon–nitrogen double bond (1.278 Å) in the *E* conformation and a short carbon–carbon single bond (1.433 Å) in the anti conformation, similar to the methyl-substituted analogue, 2,3-butanedione dihydrazone. The polymer also appears to adopt the anti-*E* conformation and so is directly comparable to *trans*-polyacetylene. Both IR and solid-state NMR analyses show the presence of hydroxy-bearing defect sites; the azines are formed by an addition–elimination condensation, and the defects arise from sites where addition occurs but the subsequent elimination does not. Polyazine can be doped with iodine to give powders with room-temperature, pressed-pellet conductivities only as high as 1×10^{-6} Ω^{-1} cm^{-1} because of the sp^3 defects found along the polymer chain. The IR spectra of the doped materials indicate that the charge carrier is a bipolaron having a nitrogen–nitrogen or carbon–carbon double bond.

Introduction

The field of conducting polymers has burgeoned in the past decade,[1] especially since the discovery that polyacetylene can be doped into a highly conductive state.[2] Since that time, a number of polymer systems have been studied, including polythiophene,[3] polypyrrole,[4] and polyaniline,[5] that have led to a better understanding of the physics and chemistry of this class of materials. Despite these advances, the currently available polymers all have deficiencies with respect to applications so that new materials must be developed and studied.

We have been investigating the chemistry and properties of the polyazines, $-[N{=}C(R){-}C(R){=}N]_x-$, which are formally isoelectronic with but topologically distinct from polyacetylene. Thus, the calculated electronic structure of polyazine was found to have narrower valence and conduction bands and a larger band gap than polyacetylene.[6] When the permethyl polyazine,[7] R = CH_3, is prepared, an environmentally stable, linear, conjugated polymer is formed that can be doped with iodine to give powders with room-temperature, pressed-pellet conductivities as high 0.1 Ω^{-1} cm^{-1}. An X-ray crystal structure of the monomer 2,3-butanedione dihydrazone coupled with an IR[7] and solid-state NMR[8] analysis of oligomers and polymers indicated that the polymer must have double bonds in the *E* conformation and single bonds in the anti conformation, i.e., analogous to *all-trans*-polyacetylene. Iodine doping of the permethyl polyazine does not alter the polymer structure but gives bipolaron charge carriers that contain either C=C or N=N moieties, as identified by IR analysis of the doped polymers.[9]

Although polyacetylene and polyazine are formally isoelectronic, the topological difference in the two polymers is significant, especially in the formation of charge carriers. *trans*-Polyacetylene can form soliton-type defects (charged or uncharged) because of the degenerate ground state of the π system:[2b] thus, the creation of a carrier does not affect the bulk of the polymer so that the mobility of the carrier should be rather high. Polyazine does not have a degenerate ground state so that creation of a soliton-type defect is energetically unfavorable since it divides the polymer into an azine portion and an azoethene portion that do not have the same energy.[6b] Instead, polyazine must form bipolaron-type defects, i.e., dications, that can act as charge carriers. This shows an important fundamental difference between polyacetylene and polyazine.

The substitution of methyl groups on the polyacetylene chain severely degrades the conductivity found in the conducting state.[2c] This result probably arises from two sources: an electronic effect of electron donation into the π system from the methyls and a geometric effect of a twisting of the chain due to steric repulsions between methyls. The previously reported studies on conducting polyazines were on the methyl-substituted derivative.[7-9] Likewise, it is anticipated that the methyl groups should have important electronic and geometric consequences on the properties of the polyazines.

The effect of the removal of the methyl groups on the chemical and physical properties of polyazine is the subject of this report. One previous communication of the synthesis of unsubstituted polyazine has appeared,[10] but details of the polymer characteristics were lacking. However, as had been earlier noted in this laboratory,[11] the unsubstituted polyazine could not be a simple linear polymer since prominent bands attributed to OH groups exist in the IR spectrum. Despite the defects found in unsubstituted polyazine, this polymer is still remarkably similar to the permethyl derivative: the all-trans conformation still appears to predominate even though there are not strong steric reasons to enforce this geometry; iodine doping is readily achieved; and the structure of the charge carrier seems to be the same type of bipolaron that is found in the permethyl derivative. The spectral evidence suggests that the defect sites are cyclic α-amino alcohols (tetrahydroxypiperazines) or tertiary α-amino dialcohols.

† University of Rhode Island.
‡ Lehigh University.

0024-9297/90/2223-4597$02.50/0

Table I
Results of Iodine Doping of Polyazine[a]

y	x	mg of PAZ	g of I_2	% C	% H	% N	% I
0.164	5.5	49.8	0.10	30.56	3.99	36.46	20.40
				(30.35)	(3.85)	(36.25)	(20.22)
0.181	6	50.6	0.15	29.78	3.88	35.11	21.88
				(29.86)	(3.73)	(35.27)	(21.96)
0.204	6	49.5	0.40	28.58	3.48	33.78	23.69
				(29.05)	(3.64)	(34.31)	(24.08)
0.304	5.5	56.0	0.50	25.91	3.24	30.92	32.06
				(25.88)	(3.28)	(30.92)	(31.92)
0.525	11	49.0	1.00	21.66	2.95	24.08	46.33
				(21.42)	(2.46)	(23.84)	(45.69)
0.738	11.5	53.0	3.00	18.45	2.64	20.45	54.64
				(18.08)	(2.07)	(20.06)	(54.23)
1.371	35	51.8	4.00	13.02	1.24	13.77	69.97
				(12.43)	(1.33)	(13.14)	(69.28)

[a] The calculated values for the elemental analyses are given in parentheses. The values for the iodine doping level (y) and the chain length (x) are estimated using 15% of a 2,3,5,6-tetrahydroxypiperazine defect and amino end groups.

In this paper we report the synthesis and physical characterization of glyoxal dihydrazone, polyazine, and iodine-doped polyazine. The X-ray crystal structure of the monomeric glyoxal dihydrazone was determined so that the physical properties of the monomer with known structure could be compared to those of the polymer, which has been isolated only as a powder. The IR and NMR spectra of the monomer and polymer are compared, especially noting the characteristics of the defect structure in the polymer. The room-temperature, pressed-pellet electrical conductivity and IR spectra of iodine-doped polymers are measured as a function of doping level. Finally, all of these properties are compared to those of the permethyl polyazine.

Experimental Section

Solutions of 40% aqueous glyoxal and hydrazine hydrate were purchased from Aldrich and used as received. Solvents were reagent grade and, unless otherwise noted, were used as received. Melting points were recorded on a Mel-Temp apparatus and are uncorrected. All elemental analyses were performed by M-H-W Laboratories, Phoenix, AZ.

$C_2H_6N_4$ (Glyoxal Dihydrazone (GDH)). The procedure used was similar to that in the literature.[12] To a stirred solution of 60.0 mL (1.2 mol) of $NH_2NH_2{\cdot}H_2O$ in an ice/acetone/salt bath was added dropwise over 60–75 min 20.0 mL (ρ = 1.270 g/mL, 0.175 mol) of 40% glyoxal in 50 mL of 95% ethanol. After the addition, the solution was stirred an additional hour. The white solid was collected and recrystallized from 95% ethanol/hydrazine hydrate (99:1 (v/v)). Long white crystals were filtered, washed with hexanes, and dried overnight under vacuum in the dark. Yield: 7.55 g, 50%, mp 98–100 °C, in agreement with the literature.[12] ^{1}H NMR (DMSO-d_6): δ 7.32 (s, 1 H), 6.58 (br s, 2 H). ^{13}C NMR: δ 139.3. Anal. Calcd for $C_2H_6N_4$: C, 27.90; H, 7.02; N, 65.08. Found: C, 27.86; H, 7.13; N, 65.36.

$(C_2H_2N_2)_x$ (PAZ). Polyazine was synthesized at three different temperatures:

Room-Temperature Preparation (RT). To 0.264 g (3.07 mmol) of GDH were added approximately 25 mL of 95% ethanol and 2 drops of glacial acetic acid in a 100-mL round-bottom flask. The stirred solution had a yellowish tint to it when 0.45 mL (3.9 mmol) of 40% glyoxal in 10 mL of 95% ethanol was added dropwise over 30 min. A precipitate formed about 10 min after the final addition of the ethanolic glyoxal solution. The solution was stirred an additional 12 h. The solution was cooled on ice, filtered, and washed with hexanes. The precipitate was placed under vacuum overnight. Yield: 0.358 g (6.62 mmol), 108%, mp 130 °C, darkening, and 208 °C, decomposing, turning black. Anal. Calcd for $C_2H_2N_2$: C, 44.44; H, 3.73; N, 51.83. Found: C, 37.46; H, 4.81; N, 46.48.

Low-Temperature Preparation (LT). A mixture of 0.50 g (5.8 mmol) of GDH, 25 mL of 95% ethanol, and 2 drops of glacial acetic acid was added to a flask at −98 °C (methanol slush). To the stirring solution was added dropwise 0.84 mL (7.4 mmol) of a 40% solution of glyoxal in 5 mL of 95% ethanol. The solution was stirred at −98 °C for an additional 2 h. The precipitate that formed was white. As the solution warmed to 0 °C, the precipitate turned yellow. The product was cooled on ice, filtered, and dried overnight under vacuum. Yield: 0.632 g (11.7 mmol), 101%, melting point as above. Anal. Calcd for $C_2H_2N_2$: C, 44.44; H, 3.73; N, 51.83. Found: C, 37.06; H, 4.37; N, 42.39.

High-Temperature Preparation (HT). A mixture of 0.462 g (5.36 mmol) of GDH, 3 drops of glacial acetic acid, and 30 mL of 95% ethanol was added to a 100-mL round-bottom flask. The solution was slightly yellow before the addition of the ethanolic glyoxal solution. To the stirred solution was added dropwise 0.78 mL (6.8 mmol) of a 40% solution of glyoxal in 10 mL of 95% ethanol. An additional 10 mL of ethanol was then added to the mixture, and the solution was heated to boiling. The reaction refluxed for 24 h. After reflux, the solution was cooled on ice, filtered, and washed with ethyl ether. The yellow product was dried under vacuum overnight. Yield: 0.608 g (11.3 mmol), 105%, melting point as above. Anal. Calcd for $C_2H_2N_2$: C, 44.44; H, 3.73; N, 51.83. Found: C, 37.26; H, 4.61; N, 45.30.

Iodine Doping. The polymers were not soluble in any common solvents, so doping was done by stirring a mixture of iodine and PAZ in a solvent in which the iodine was soluble. Typically, 50 mg of PAZ (all from the room-temperature preparation) was added to a 250-mL Erlenmeyer flask, a weighed amount of iodine was added to the flask, and the flask was corked; after about an hour, 25 mL of chloroform was added to the flask, and the solution was vigorously stirred for an additional 24 h. The gas-phase pretreatment of the PAZ was important for achieving maximum doping for any given amount of iodine used. After the stirring was complete, the product was vacuum filtered and washed with 25 mL of chloroform followed by as much cyclohexane as was required to remove the unreacted iodine. Table I gives the analytical results and experimental conditions for all of the iodine-doped materials prepared.

Instrumentation. IR spectra were run between 4000 and 600 cm^{-1} as KBr pellets on a Perkin-Elmer 281B spectrometer. All of the spectra were referenced to polystyrene. Solid-state NMR spectra were obtained at Lehigh University on a General Electric GN-300 NMR instrument operating at 75.4 MHz for ^{13}C. The Doty Scientific, Inc., 7-mm probe utilized sapphire rotors and Kel-F end caps containing a sample volume of up to 0.35 cm^3. Spectra were obtained with cross polarization[13] and magic-angle sample spinning.[14] Spinning speeds were measured between 3.7 and 5.4 kHz. Typical conditions included a single cross polarization contact time of 2 ms and an acquisition time of 40 ms. Signal averaging of 128 to approximately 5000 transients improved the signal-to-noise (S/N) ratio, with a 4–6-s recycle time. Exponential line broadening equivalent to 100 Hz was applied before zero-filling and Fourier transformation (FT). Maximum radio-frequency field strengths were 1.4 and 4.2 mT for protons and carbon. Chemical shifts are relative to TMS referenced to external adamantane, with an estimated error of ±0.2 ppm[15] for sharp, well-defined peaks. For the broader resonances, chemical

shift errors are larger. Solution NMR were obtained on a Bruker AM-300 instrument operating at 300 MHz for protons and 75.4 MHz for ^{13}C.

X-ray Crystallography. Crystals suitable for diffraction were grown by slow evaporation of an ethanol/hydrazine hydrate solution. The data crystal measured approximately 0.6 × 0.8 × 1.0 mm. Lattice parameters a = 7.744 (4) Å, b = 4.113 (1) Å, c = 8.063 (4) Å, and β = 115.66 (3)° were determined by a least-squares fit of 25 carefully centered reflections between 19 and 33° 2θ. An approximate density measurement of 1.23 g cm^{-3} (determined by flotation in CCl_4 diluted with C_6H_{14}) suggested that two molecules of composition $C_2H_6N_4$ occupied the unit cell with a volume of 231.49 (16) Å^3 and calculated density 1.235 g cm^{-3}. Systematic absences[16] ($0k0$, $k = 2n + 1$; $h0l$, $h = 2n + 1$) uniquely defined the space group $P2_1/a$. Since the multiplicity of this space group is 4, the molecule must lie on a crystallographic center of symmetry.

The structure was solved by direct methods[17] and refined[18] successfully in space group $P2_1/a$, confirming the space group assignment. A total of 820 reflections, of which 683 were unique, with $3.5 < 2\theta < 60°$ and hkl minima and maxima of 0,0,-12 and 11,6,12, respectively, were collected at room temperature with a Nicolet R3M/E autodiffractometer using graphite-monochromated Mo Kα radiation (λ = 0.71073 Å) and variable-speed (2.93-29.30° min^{-1}) 2θ scans, with three standard reflections (003, 020, 600) measured every 97 reflections. There was no evidence of decay in the standard reflections during data collection. The intensities were corrected for Lorentz and polarization effects, a profile anlaysis was applied, but no correction for absorption was made. The carbon and nitrogen atoms were refined anisotropically, while hydrogen atoms were refined isotropically, using all unique data. Refinement converged resulting in final agreement factors $R(F)$ = 0.056 and $R_w(F)$ = 0.059 using a fixed weighting scheme, $W = 1.0000/\sigma^2(F) + 0.0001(F)^2$, where $\sigma(F)^2$ is from counting statistics.

Results

Synthesis. The general reaction we have used to prepare polyazines is a condensation of an α,β-dicarbonyl with an α,β-dihydrazone with acid catalysis.

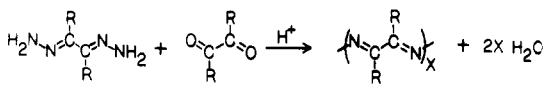

This general scheme is appropriate for R = H as well. However, the glyoxal used as the dicarbonyl is supplied as a 40% aqueous solution and does not exist as a dialdehyde; rather, the bulk of the glyoxal oligomerizes in solution to give primarily a bicyclic trimeric dihydrate:

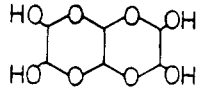

This form of the glyoxal can react as a dialdehyde, as evidenced by the formation of the glyoxal dihydrazone, but the addition–elimination condensation reaction to form the imine bond is not as facile as in the butanedione case. In fact, in the reaction to form the glyoxal dihydrazone, if the glyoxal is added to the hydrazine solution too quickly, an unidentified white product that is not the desired dihydrazone can be isolated. Elucidation of this alternate chemistry is in progress.

The other effect of the bicyclic glyoxal structure is that when the polymerization is occurring, three glyoxal units are in proximity of the amine end of the growing chain. This means that a high local concentration of glyoxal units is always present at the attacking site, allowing for the possibility of multiple attack at the amine nitrogen. If an amine nitrogen reacts with more than one glyoxal unit, thereby removing both hydrogens on the nitrogen atom, elimination of water is prevented, allowing for defect formation. This process is kinetic in nature, so temperature variation should affect the results of this reaction.

Table II
End-Group Analysis Using Elemental Analysis

	% C	% H	% N
$-(N{=}CH{-}CH{=}N)_x-$ (ideal structure)	44.44	3.73	51.80
low-temp prep, found	37.06	4.37	42.39
$H_2N[C_2H_2N_2(C_4H_8N_2O_4)_{0.24}]_5NH_2$	37.03	4.96	42.02
room-temp prep, found	37.46	4.81	46.48
$H_2N[C_2H_2N_2(C_4H_8N_2O_4)_{0.15}]_{4.5}NH_2$	37.45	4.94	46.10
high-temp prep, found	37.26	4.61	45.30
$H_2N[C_2H_2N_2(C_4H_8N_2O_4)_{0.17}]_{4.5}NH_2$	37.28	4.96	45.16

The synthesis of PAZ at various temperatures demonstrates the effect of the acetal form of the glyoxal. When the polymer is formed at low (-98 °C) temperatures, the polymer does not initially precipitate in the characteristic yellow color of polyazine; only upon warming does sufficient dehydration occur to cause the product to turn yellow, indicative of conjugation. Even after warming, the product contains a large percentage of oxygen, as determined by the elemental analysis. Polymerization at room temperature or in refluxing ethanol gives essentially the same product, with a much lower oxygen content than that found in the low-temperature preparation. Different preparations of polymer at a given temperature also can give different oxygen content; it appears that the rate of addition of the glyoxal to the reacting solution has some influence on the nature of the product. Investigation of the details of the polymerization reaction is in progress.

Because of the large amount of water present in the glyoxal reactant, only short-chain polymers are formed and elemental analysis can be effectively used in an end-group analysis to estimate chain lengths. The end groups in polyazine can be either carbonyl or amino moieties; in a defect-free polymer, the C/N ratio identifies the predominant end group since a C/N > 1 indicates that the carbonyl is the dominant terminator while a C/N < 1 implies that amino groups prevail at chain ends. The elemental analyses of all of the polymers prepared here are best fit using amino end groups. The oxygen content found in the polymer was modeled with tetrahydroxypiperazine (as inferred from the spectroscopic results) as the oxygen source. The results of the modeling for the elemental analyses are found in Table II. The polyazines synthesized here have chain lengths on the order of five monomer units, much shorter than that found in the permethyl polyazines.[7] As indicated by the color changes occurring during synthesis, the low-temperature preparation has a much higher defect concentration than the other two polymers, which are effectively identical. These findings must be considered as quite approximate, since the fitting procedure is moderately sensitive relative to the typical error in analytical results.

The polymer can be doped with iodine to any iodine content desired up to about 1.4 I atoms per monomer unit. In order to achieve the highest levels of doping, however, it is necessary to allow the I_2 and PAZ to react in the absence of solvent for a period of time (we previously reported an upper doping limit of about 0.3 I atom per repeat unit when no pretreatment was used[11b]). Subsequent addition of solvent allows the completion of the reaction. Presumably this gas-phase pretreatment of the doping reaction only attacks the surface of the PAZ powder, but this may be important toward opening channels to let the iodine into the bulk of the polymer to give complete reaction. The amount of iodine in the maximally doped

Table III
Final Positional and Thermal Parameters for All Atoms and Isotropic Thermal Parameters for the Hydrogen in the Asymmetric Unit of Glyoxal Dihydrazone[a]

atom	x/a	y/b	z/c	$U \times 10^4$	$U_{11} \times 10^4$	$U_{22} \times 10^4$	$U_{33} \times 10^4$	$U_{12} \times 10^4$	$U_{13} \times 10^4$	$U_{23} \times 10^4$
Cl	0.08963 (12)	0.03320 (25)	0.07717 (12)		445 (5)	598 (6)	505 (5)	−7 (4)	240 (4)	35 (4)
N1	0.09452 (11)	0.19489 (25)	0.21444 (10)		465 (5)	717 (6)	486 (5)	−32 (4)	223 (4)	3 (4)
N2	0.27180 (14)	0.23834 (35)	0.36139 (13)		521 (5)	1023 (9)	521 (5)	−78 (5)	187 (5)	−95 (5)
H1	0.20814 (180)	−0.04259 (295)	0.07503 (166)	616 (30)						
H2	0.37006 (227)	0.23761 (424)	0.32441 (182)	856 (39)						
H3	0.27067 (221)	0.41470 (441)	0.42508 (245)	861 (44)						

[a] The isotropic temperature factor is $\exp[-U \sin^2 \theta/8\lambda^2\pi^2]$, where $U = B/8\pi^2$. The complete anisotropic temperature factor is $\exp[-2\pi^2(U_{11}h^2a^{*2} + U_{22}k^2b^{*2} + U_{33}l^2c^{*2} + 2U_{12}hka^*b^* + 2U_{13}hla^*c^* + 2U_{23}klb^*c^*)]$.

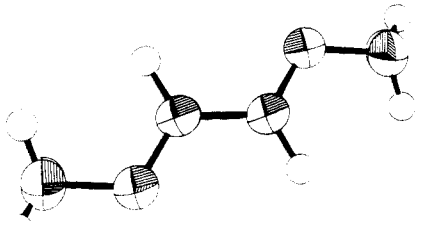

Figure 1. ORTEP drawing of glyoxal dihydrazone. The thermal ellipsoids are drawn at the 50% probability level.

polymer is similar to the doping levels achievable in permethyl polyazine.[7]

X-ray Crystallography. The molecule crystallizes in the *s-trans* (single bond anti, double bonds *E*) conformation with the C–C bond lying on the crystallographic inversion center as shown in Figure 1. Final positional and thermal parameters are given in Table III; bond lengths and bond angles are given in Table IV. The C–C (1.433 (2) Å) and C–N1 (1.278 (1) Å) bonds are shorter than the range of comparable bonds, 1.462–1.483 and 1.282–1.306 Å, respectively, in 2,3-butanedione dihydrazone (**2**),[7] 2,3-butanedione bis(2′-nitrophenylhydrazone) (**3**),[19] (*E,E*)-2,3-butanedione bis(4′-nitrophenylhydrazone) (**4**),[20] and dimethylglyoxal bis(guanylhydrazone) (**5**),[21] possibly a result of decreased steric strain in the title compound **1** compared to **2**–**5**. The N1–N2 bond length (1.383 (1) Å) is shorter than the analogous bond in **2** (1.387 (1) Å) but, like **2**, is longer than comparable bonds (1.356 (2)–1.371 (8) Å) in **3**–**5**.

The heavy atoms of glyoxal dihydrazone are planar with the largest deviation from the least-squares plane being less than 0.02 Å. The imine hydrogen, H1, lies 0.069 Å off of this plane. The planarity of this molecule and short C–C and C=N bond lengths are strong indicators of the large amount of conjugation along the molecular backbone. In comparison to 2,3-butanedione dihydrazone, the backbone bonds are all significantly shorter in glyoxal dihydrazone and there is less deviation from planarity in the unsubstituted molecule.[7]

Molecules of **1** form two hydrogen-bonded networks, N1···H2($-{}^1/_2+x,{}^1/_2-y,z$) (2.28 (2) Å) and N2···H3($x,-1+y,z$) (2.31 (2) Å) as shown in the packing diagram in Figure 2. Both nitrogen atoms of GDH are involved in the hydrogen-bonding network. The N–H–N angles are 172° for the N1···H2–N2 bond and 160° for the N2···H3–N2 interaction, typical of hydrogen bonds in these type systems.[7,19-21] In 2,3-butanedione dihydrazone there is no close H-bonded contact to the imine nitrogens, in contrast to what is observed for GDH, mainly due to the steric repulsion afforded by the methyl substituents on the carbon atoms, an effect not available to GDH.

IR Spectroscopy. The infrared spectrum of glyoxal dihydrazone is dominated by strong N–H vibrations at 3339 (antisymmetric stretch), 3158 (symmetric stretch), 1628 (internal deformation), and 636 cm^{-1} (rock), similar to those found in the IR spectrum of 2,3-butanedione dihydrazone.[7] An intense peak is found at 1069 cm^{-1} that is assigned to the N–N stretch (the N–N stretch is found at 1098 cm^{-1} in hydrazine[22]). Also of note is the imine vibration at 1572 cm^{-1}, quite low for typical imine stretches, which is in accord with the idea that a fair amount of conjugation exists even in this monomeric azine, as suggested above from the crystal structure. The imine vibration in butanedione dihydrazone is found at 1560 cm^{-1}, significantly lower than in GDH, but in accord with the bond lengths found in the single-crystal X-ray analysis (1.278 Å for GDH and 1.291 Å for 2,3-butanedione dihydrazone).

Figure 3 compares the IR spectrum of GDH with PAZ (room-temperature preparation; the IR spectra of the polymers at the three different temperatures are virtually identical). The polymer spectrum has a broad udder-shaped absorption centered at 3400 cm^{-1} that is assigned to a combination of OH and NH vibrations. The band shape suggests OH vibrations but two small features in essentially the same positions as the NH_2 vibrations of GDH also denote the presence of NH stretching. This is in accord with the short-chain nature of this material as found from the elemental analysis. The breadth of all the IR peaks is attributed to a fairly wide distribution of molecular weights in this polymer; this is in direct contrast to permethyl polyazine, which has sharp IR peaks and a narrow molecular weight distribution.[7]

The IR spectrum of PAZ has three major features below 2000 cm^{-1} located at 1602, 1542, and 1128 cm^{-1}. The 1602-cm^{-1} peak is due to isolated imines near chain defects. The strong absorption at 1542 cm^{-1} is assigned to an imine stretch in the conjugated regions of the polymer. This is 30 cm^{-1} lower in energy than the analogous vibration found in the monomer GDH, indicating the increased conjugation found in the polymer. This is counter to what is found in the permethyl polyazine, where the imine vibration in the polymer is found 25 cm^{-1} to higher energy than the corresponding monomer, an effect due to the methyl substitution. The feature found at 1128 cm^{-1} is attributed to two sources: the N–N vibration along the chain and the C–O stretch at hydration sites.

The IR spectra of a number of iodine-doped polyazines are shown in Figure 4. Two new features are noted in these spectra: a broad, intense absorption centered near 4000 cm^{-1} and a "narrow" peak at 1490 cm^{-1}. Both peaks grow in relative intensity as the doping level increases. The peak at 4000 cm^{-1} is assigned to an absorption of the free electron in the conduction band.[9] The peak at 1490 cm^{-1} is of a vibrational nature, is in the double-bond region, and is associated with the charge carrier. A similar peak has been observed in the IR spectrum of the iodine-doped permethyl polyazine at 1505 cm^{-1},[7,9] and this absorption has

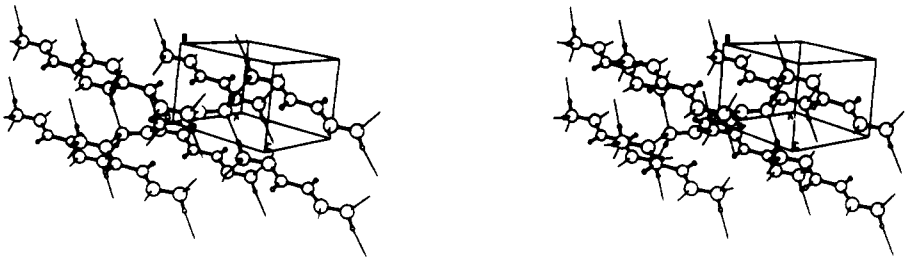

Figure 2. ORTEP packing diagram of glyoxal dihydrazone. The thermal ellipsoids are drawn at the 50% probability level.

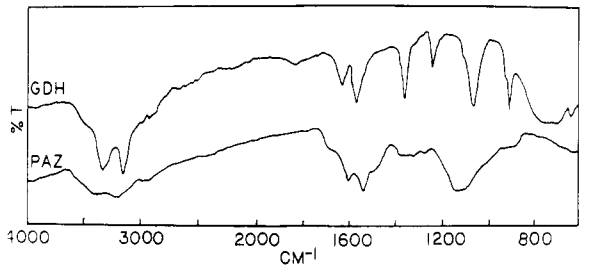

Figure 3. IR spectra of glyoxal dihydrazone (GDH) and polyazine (PAZ) taken between 600 and 4000 cm^{-1} as KBr pellets.

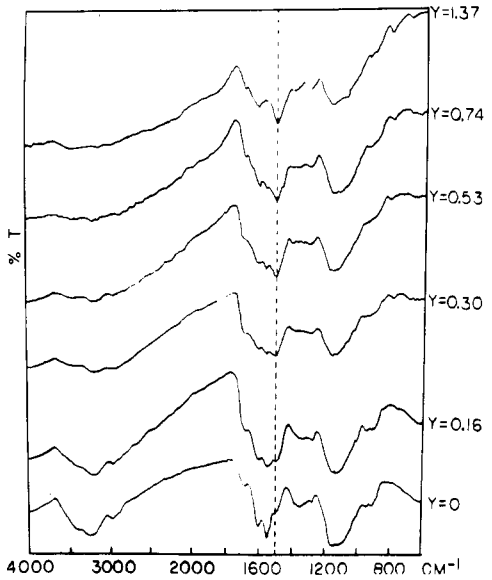

Figure 4. IR spectra of iodine-doped polyazine for various doping levels, y, taken between 600 and 4000 cm^{-1} as KBr pellets. The dashed line denotes the position of the doping-induced vibrational band that grows with increasing doping level.

been assigned to either a C=C or N=N vibration found in a bipolaron carrier of the type

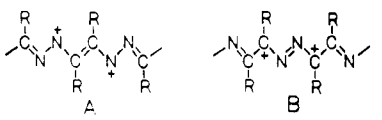

Either of these structures can account for the 1490-cm^{-1} peak based on currently available evidence.

^{13}C NMR Spectroscopy. The solution ^{13}C NMR spectrum of glyoxal dihydrazone has a single peak at 139.3 ppm; this compares to 147.5 ppm in solution and 147.3 ppm in the solid state for butanedione dihydrazone. This is in agreement with the somewhat smaller delocalization found in GDH from both the IR and the crystallographic studies.

The solid-state ^{13}C NMR spectra of PAZ prepared at three different temperatures are shown in Figure 5. The major absorptions in all three spectra are the same, found

Table IV
Bond Lengths (Å) and Bond Angles (deg) in Glyoxal Dihydrazone

	Bond Lengths		
C1–N1	1.2777 (15)	N1–N2	1.3827 (32)
C1–H1	0.9764 (149)	N2–H2	0.9297 (196)
C1–C1′	1.4332 (32)	N2–H3	0.8910 (193)
	Bond Angles		
H1–C1–C1′	119.22 (75)	N1–N2–H2	111.81 (88)
N1–C1–C1′	120.37 (25)	N1–N2–H3	110.19 (127)
N1–C1–H1	120.40 (81)	H2–N2–H3	113.65 (161)
C1–N1–N2	117.10 (25)		

at 161.7, 136.5, and 75.3 ppm, and all are quite broad. The peaks at 75.3 ppm are of major interest, since they signal sp^3 carbons in the polymers, indicating that these polyazines are not totally conjugated along the entire chain. This is quite different from the permethyl polyazine that has no drastic conjugation breaks along the macromolecular chain.[8] The 75.3 ppm resonance can be assigned to tetrahydroxypiperazines (THP) as suggested by Cao and Li[10]

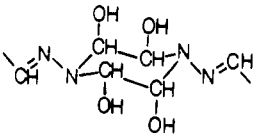

This fits the IR data and is consistent with the elemental analysis, as shown in Table II. Simple additivity rules imply a chemical shift of about 100 ppm for the sp^3 carbons in the piperazine ring,[24] but we used the following model[25] and measured the solution ^{13}C NMR peaks at 72.4, 72.6, 77.5, and 77.6 ppm, consistent with the broad 75.3 ppm peak found in the PAZ solid-state NMR spectrum.

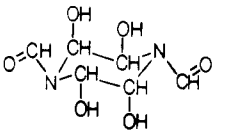

Another possibility is that two glyoxals attack an amino end group but do not ring close. If this situation arises, a tertiary α-amino dialcohol is formed that can act as a

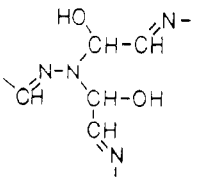

cross-linking defect in the polymer. Two sp^3 sites still remove the conjugation of the polyazine backbone so that delocalized segments of the π system still can be of varying lengths, leading to the broad IR and NMR spectra and the presence of two types of imine bonds.

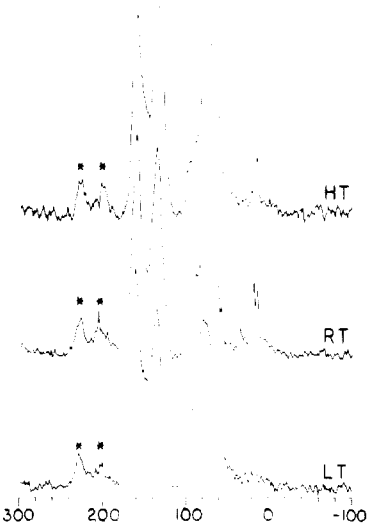

Figure 5. Solid-state ^{13}C NMR spectra of polyazine prepared at low temperature (LT), room temperature (RT), and high temperature (HT). Stars denote rotational sidebands.

The peaks at 136.5 and 161.7 ppm are assigned to imine carbons. The lower field peak is assigned to imines in the middle of a long, highly conjugated segment, while the higher field peak is assigned to imines at the ends of the conjugated segments or not in conjugation with the π system. The resonance position for the end-of-segment imines is about the same as the chemical shift for the monomer, GDH (139.3 ppm), consistent with our assignment. The peaks for the middle-of-segment imines are shifted about 25 ppm downfield from the end imines, showing the large degree of conjugation in these portions of the polymer, again in accord with the IR imine stretches. This 25 ppm shift is much larger than observed in the permethyl polyazine, where the shift from end groups to bulk polymer was found to be only about 8 ppm.[8]

The difference in the NMR spectra between the polymers prepared at different temperatures lies in the minor peaks. The sample prepared at low temperature has only the three major peaks with significant intensity while the other two samples have peaks at 57.9, 35.2, 18.9, and 14.4 ppm. The pair of peaks at 57.9 and 18.9 ppm are due to the solvent, ethanol, trapped in the lattice. Permethyl polyazine also traps solvent in the lattice that can be observed in both the NMR and IR.[8b] The peak at 14.4 ppm is assigned to the methyl groups of diethyl acetal end groups; the hydrated carbonyl end group readily reacts with ethanol to form the acetal. The diethyl acetal of formaldehyde was used as a model compound to make this assignment; we find resonances at 89.1, 63.4, and 15.3 ppm for diethoxymethane. If the 14.4 ppm peak in the polymer is due to acetal end groups, then peaks should also be found near 63 and 89 ppm. Indeed, shoulders exist on both sides of the large 75.3 ppm peak, consistent with the end-group assignment. However, it must be noted that some (probably most) of the intensity in these shoulders is due to rotational sidebands from the 136.5 and 161.7 ppm peaks. The presence of acetal end groups is in direct contrast to the conclusions of the elemental analysis, which suggested predominantly amino end groups. Apparently, most end groups are amine but a sufficient number are acetal that are detected by the NMR experiment. The last minor peak at 35.2 ppm is unassigned; we can find no reasonable structure consistent with these preparative conditions that can account for this peak.

Electrical Conductivity. The electrical conductivity of pressed pellets of the iodine-doped species were measured. Only the highest doped material ($y = 1.4$) had a conductivity within the limits of our instrument with a room-temperature conductivity of $\sigma = 1 \times 10^{-6}\ \Omega^{-1}\ cm^{-1}$. This is 5 orders of magnitude lower than the conductivity found in the permethyl polyazine. Since the IR spectra of the iodine-doped PAZ show the characteristic vibration of the charge carrier, the defect sites must prevent passage of the bipolaron from one conjugated segment to the next. Either type of defect proposed could realize such behavior.

Discussion

The combination of elemental analysis, IR spectroscopy, and solid-state NMR spectroscopy gives a complete picture of the structure of polyazine. The polymer is primarily a linear conjugated chain of head-to-head-linked imine moieties; however, about 15% of the repeat units have tetrahydroxypiperazine defect sites. The end groups of the polyazine synthesized in ethanol solvent are primarily amine groups but with some diethoxy acetals. The double bonds are highly conjugated and in the *E* conformation while the single bonds are in the anti conformation, so that polyazine in the defect-free regions is, geometrically, exactly analogous to *trans*-polyacetylene. The defect sites serve to limit the length of the conjugated segments, but both the IR and NMR show that extended portions of the π system of the polymer are indeed delocalized.

The suggestion of Cao and Li[10] that the defect sites are 2,3,5,6-tetrahydroxypiperazines seems reasonable. This structure has a number of hydroxyl groups that account for the strong IR band above 3200 cm^{-1} and for the oxygen content of the polymer. Further, this structure is consistent with the solid-state ^{13}C NMR peak found near 75 ppm. It also seems possible that such a cyclic structure is chemically feasible since the reactant glyoxal exists in a bicyclic form in aqueous solution. This type of defect allows that the polymer is still primarily one-dimensional but a "bubble" exists along the chain, putting a substantial conjugation break in the π system of the polymer. The other type of defect considered was a tertiary α-amino dialcohol. This structure introduces the possibility of cross-linking into the polymer as well as saturation along the electronic backbone. Undoubtedly, both types of defects exist but the elemental analysis results were well fit by assuming all THP defects. This is also consistent with the low conductivities found for the iodine-doped polyazines. We intend to try to resolve this question of the types of defects by an examination of the solid-state ^{15}N NMR spectra of a series of polyazines and model compounds. These results will be reported elsewhere.

If the defect could be removed from the polymer, it seems likely that the conductivity could be improved substantially. In order to do this, the condensation polymerization reaction will need to use monomeric glyoxal in relatively low dilution. One possible way to accomplish this is to use the bisulfite addition product of glyoxal as the dialdehyde source (this will decompose under acidic conditions) in the absence of water so that the bicyclic trimeric dihydrate of glyoxal cannot form. This may have the additional benefit of leading to higher molecular weight polymers. Efforts toward synthesizing the defect-free unsubstituted polyazine are in progress.

Acknowledgement is made to the donors of the Petroleum Research Fund, administered by the American Chemical Society, for support of this work. J.E.R. acknowledges a grant from the NSF Division of Materials Science Solid State Chemistry Program (DMR-8553275).

Supplementary Material Available: Table of structure factors for glyoxal dihydrazone (5 pages). Ordering information is given on any current masthead page.

References and Notes

(1) Skotheim, T. A., Ed. *Handbook of Conducting Polymers*; Marcel Dekker: New York, 1986.

(2) (a) Fincher, C. R., Jr.; Ozaki, M.; Heeger, A. J.; MacDiarmid, A. G. *Phys. Rev. B* **1979**, *19*, 4140. (b) Su, W. P.; Schrieffer, J. R.; Heeger, A. J. *Phys. Rev. Lett.* **1979**, *42*, 1698. (c) Chien, J. C. W.; Wnek, G. E.; Karasz, F. E.; Hirsch, J. A. *Macromolecules* **1981**, *14*, 479. (d) Baughman, R. H.; Moss, G. *J. Chem. Phys.* **1982**, *77*, 6321. (e) Baughman, R. H.; Murthy, N. S.; Miller, G. G. *J. Chem. Phys.* **1983**, *79*, 515. (f) Moraes, F.; Chen, J.; Chung, T.-C.; Heeger, A. J. *Synth. Met.* **1985**, *11*, 271. (g) Jeyadev, S.; Conwell, E. M. *Phys. Rev. B* **1986**, *33*, 2530. (h) Chien, J. C. W.; Schen, M. A. *Macromolecules* **1986**, *19*, 1042. (i) Basescu, N.; Liu, Z.-X.; Moses, D.; Heeger, A. J.; Naarmann, H.; Theophilou, N. *Nature* **1987**, *327*, 403. (j) Roth, S.; Bleier, H. *Adv. Phys.* **1987**, *36*, 385. (k) Naarmann, H.; Theophilou, N. *Synth. Met.* **1987**, *22*, 1. (l) Swager, T. M.; Dougherty, D. A.; Grubbs, R. H. *J. Am. Chem. Soc.* **1988**, *110*, 2973.

(3) (a) Tourillon, G.; Garnier, F. *J. Phys. Chem.* **1983**, *87*, 2289. (b) Pfluger, P.; Street, G. B. *J. Chem. Phys.* **1984**, *80*, 544. (c) Tourillon, G.; Gourier, D.; Garnier, P.; Vivien, D. *J. Phys. Chem.* **1984**, *88*, 1049. (d) Chung, T.-C.; Kaufman, J. H.; Heeger, A. J.; Wudl, F. *Phys. Rev. B* **1984**, *30*, 702. (e) Davidov, D.; Moraes, F.; Heeger, A. J.; Wudl, F.; Kim, H.; Dalton, L. R. *Solid State Commun.* **1985**, *53*, 497. (f) Chen, J.; Heeger, A. J.; Wudl, F. *Solid State Commun.* **1986**, *58*, 251. (g) Frommer, J. E. *Acc. Chem. Res.* **1986**, *19*, 2. (h) Hotta, S.; Rughooputh, S. D. D. V.; Heeger, A. J.; Wudl, F. *Macromolecules* **1987**, *20*, 212. (i) Hess, B. C.; Shinar, J.; Ni, Q.-X.; Vardeny, Z.; Wudl, F. *Synth. Met.* **1989**, *28*, C365.

(4) (a) Brédas, J. L.; Scott, J. C.; Yakushi, K.; Street, G. B. *Phys. Rev. B* **1984**, *30*, 1023. (b) Pfluger, P.; Gubler, U. M.; Street, G. B. *Solid State Commun.* **1984**, *49*, 911. (c) Brédas, J. L.; Thémans, B.; Fripiat, J. G.; André, J. M.; Chance, R. R. *Phys. Rev. B* **1984**, *29*, 6761. (d) Rühe, J.; Ezquerra, T. A.; Wegner, G. *Synth. Met.* **1989**, *28*, C177.

(5) (a) MacDiarmid, A. G.; Chiang, J.-C.; Halpern, M.; Huang, W.-S.; Mu, S.-L.; Somasiri, N. L. D.; Wu, W.; Yaniger, S. I. *Mol. Crystl. Liq. Cryst.* **1985**, *121*, 173. (b) Paul, E. W.; Ricco, A. J.; Wrighton, M. S. *J. Phys. Chem.* **1985**, *89*, 1441. (c) Hjertberg, T.; Salaneck, W. R.; Lundstrom, I.; Somasiri, N. L. D.; MacDiarmid, A. G. *J. Polym. Sci., Polym. Lett. Ed.* **1985**, *23*, 503. (d) McManus, P.; Yang, S. C.; Cushman, R. J. *J. Chem. Soc., Chem. Commun.* **1985**, 1556. (e) Euler, W. B. *Solid State Commun.* **1986**, *57*, 857. (f) Chiang, J.-C.; MacDiarmid, A. G. *Synth. Met.* **1986**, *13*, 193. (g) Stafstrom, S.; Brédas, J. L.; Epstein, A. J.; Woo, H. S.; Tanner, D. B.; Huang, H. S.; MacDiarmid, A. G. *Phys. Rev. Lett.* **1987**, *59*, 1464. (h) MacDiarmid, A. G.; Chiang, J. C.; Richter, A. F.; Epstein, A. J. *Synth. Met.* **1987**, *18*, 285. (i) Shacklette, L. W.; Wolf, J. F.; Gould, S.; Baughman, R. H. *J. Chem. Phys.* **1988**, *88*, 3955. (j) Angelopoulos, M.; Asturias, G. E.; Ermer, S. P.; Ray, A.; Scherr, E. M.; MacDiarmid, A. G.; Akhtar, M.; Kiss, Z.; Epstein, A. J. *Mol. Cryst. Liq. Cryst.* **1988**, *160*, 151.

(6) (a) Euler, W. B.; Hauer, C. R. *Solid State Commun.* **1984**, *51*, 473. (b) Euler, W. B. *J. Phys. Chem.* **1987**, *91*, 5795.

(7) Hauer, C. R.; King, G. S.; McCool, E. L.; Euler, W. B.; Ferrara, J. D.; Youngs, W. J. *J. Am. Chem. Soc.* **1987**, *109*, 5760.

(8) (a) Euler, W. B.; Roberts, J. E. *Synth. Met.* **1989**, *29*, E545. (b) Euler, W. B.; Roberts, J. E. *Macromolecules* **1989**, *22*, 4221.

(9) Euler, W. B. *Solid State Commun.* **1988**, *68*, 291.

(10) Cao, Y.; Li, S. *J. Chem. Soc., Chem. Commun.* **1988**, *937*.

(11) (a) Hauer, C. R. Master's Thesis, University of Rhode Island, 1985. (b) Euler, W. B.; Gill, B. C. Materials Research Society Meeting, November 1989.

(12) Bayer, E.; Breitmaier, E.; Schurig, V. *Chem. Ber.* **1968**, *101*, 1594.

(13) Pines, A.; Gibby, M.; Waugh, J. S. *J. Chem. Phys.* **1973**, *59*, 569.

(14) Schaefer, J. F.; Stejskal, E. O. *J. Am. Chem. Soc.* **1976**, *98*, 1031.

(15) Earl, W. L.; VanderHart, D. L. *J. Magn. Reson.* **1982**, *48*, 35.

(16) Six of 85 reflections in the set *h*0*l* ($h = 2n + 1$) were above 3σ, but the structure could not be successfully refined in either the $P2_1$ or $P2_1/m$ space groups.

(17) Main, P.; Hull, S. E.; Lessinger, L.; Germain, G.; Declercq, J.-P.; Woolfson, M. M. *MULTAN81, A System of Computer Programs for the Automatic Solution of Crystal Structures from Diffraction Data*; University of York: York, England, 1981.

(18) Sheldrick, G. M. *SHELX-76, A Program for Crystal Structure Determination*; Cambridge University: Cambridge, England, 1976.

(19) Edwards, J. W.; Hamilton, W. C. *Acta Crystallogr., Sect. B* **1972**, *28*, 1362.

(20) Wiley, G. R.; Drew, M. G. B. *Acta Crystallogr., Sect. C* **1983**, *39*, 403.

(21) Wiley, G. R.; Drew, M. G. B. *Acta Crystallogr., Sect. C* **1985**, *41*, 589.

(22) Druig, J. R.; Bush, S. F.; Mercer, E. E. *J. Chem. Phys.* **1966**, *44*, 4238.

(23) Euler, W. B. *Chem. Mater.* **1990**, *2*, 209.

(24) Abraham, R. J.; Fisher, J.; Loftus, P. *Introduction to NMR Spectroscopy*; Wiley: Chichester, 1988.

(25) Vail, S. L.; Moran, C. M.; Barker, R. H. *J. Org. Chem.* **1965**, *30*, 1195.